

Dopant local bonding and electrical activity near Si(001)-oxide interfaces

Zhiyong Zhou, Michael L. Steigerwald, Richard A. Friesner, and Louis Brus
*Department of Chemistry and Center for Electron Transport in Molecular Nanostructures,
 Columbia University, New York, New York 10027*

Mark S. Hybertsen^{a)}

*Department of Applied Physics and Applied Mathematics and Center for Electron Transport
 in Molecular Nanostructures, Columbia University, New York, New York 10027*

(Received 5 May 2005; accepted 23 August 2005; published online 7 October 2005)

Electronic structure calculations based on a density-functional approach have been performed for P, As, B, and Al substitutional dopants near the Si(001)-oxide interface. The structures are geometrically optimized for each charge state. P and As geometries show a strong distortion when neutral, and regain tetrahedral local bonding when ionized. This geometry change creates an activation barrier for the release of the electron. Distorted neutral dopants may react with hydrogen during the forming gas interface passivation. In contrast, B and Al show tetrahedral bonding for all charge states. All four neutral dopants show substantial energy gain upon formation of dimer complexes near the interface. Neutral B is significantly more stable when bonded to two O atoms at the interface, while neutral P is more stable bonded to four Si atoms adjacent to the interface. © 2005 American Institute of Physics. [DOI: 10.1063/1.2071447]

This paper concerns the local chemical bonding and electrical activity of dopants within a few silicon layers of the Si(001)-oxide interface. The control of the distribution of electrically active dopants in the Si channel near the gate oxide is a critical issue in modern Si field-effect transistors (FETs).¹ P and As dopants are known to thermally diffuse and preferentially segregate at the oxide interface in the high-temperature anneal that follows dopant ion implantation.² Extensive experimental work shows that up to a monolayer of dopants are trapped in the first layer of Si, just below the Si atom layer that is bonded to oxygen.³ Auger electron spectroscopy (AES) data show that the dopants are neutral and thus have not liberated a hole or electron into the Si channel.⁴ We now address the local structure near the dopant based on relative energetic stability and electrical activity as a function of dopant position near this interface.

Extensive testing has shown that electronic structure calculations with the hybrid B3LYP functional in density-functional theory, which combines exact Hartree-Fock exchange with the generalized gradient approximation, quantitatively reproduce a wide range of chemical-bonding behavior in molecules and crystals. Experimental bond energies and ionization potentials in a standard molecular test set are reproduced with residual errors of 0.13 eV, about 10% of the residual errors found with the commonly used local-density approximation (LDA).⁵ In crystalline solids, hybrid functionals reproduce the band gap of many complex mixed-valence transition-metal oxide crystals^{6,7} and improves on the LDA band gap for semiconductors.⁶ We use the JAGUAR 5.0 code⁸ with the Los Alamos lav3p** pseudopotential atom-centered basis set⁹ for Si, P, As, and Al; the 6-31G** all-electron basis set is used for B, H, and O.

In the literature a range of interface structures have been proposed and partially characterized.^{4,10,11} Figure 1(a) shows

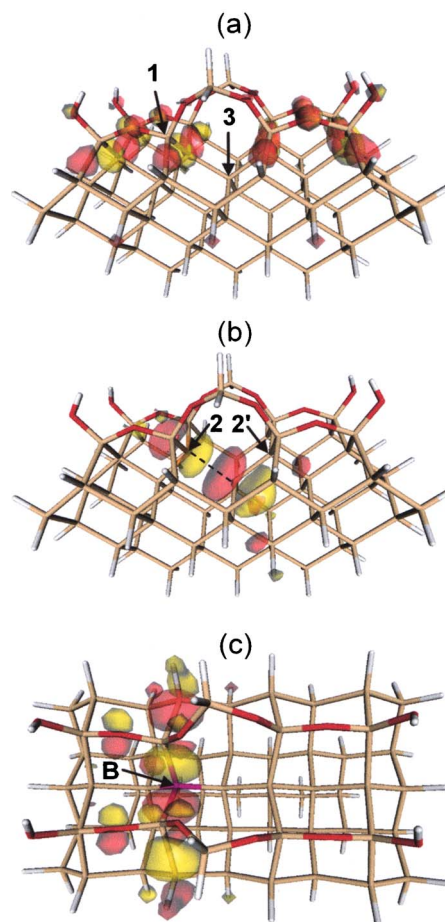


FIG. 1. (Color online) Cluster model for the Si(001)-oxide interface, $\text{Si}_{62}\text{H}_{52}\text{O}_{12}$. Side view, (a) and (b); top view, (c). Oxygen indicated in red; hydrogen in white. Specific positions enumerated for reference. Isosurface plot of the highest-occupied molecular orbital of (a) the undoped parent, (b) the relaxed neutral $\text{Si}_{61}\text{PH}_{52}\text{O}_{12}$ with P at site indicated by the arrow as 2 and showing a broken bond highlighted by the dashed line, and (c) the relaxed neutral $\text{Si}_{61}\text{BH}_{52}\text{O}_{12}$ with B in the site indicated by the arrow.

^{a)}Electronic mail: msh2102@columbia.edu

$\text{Si}_{62}\text{H}_{52}\text{O}_{12}$ —a finite section of the flat, dimerized, oxygen-bridged stripe phase model.¹² This interface has no defects or dangling bonds passivated with H. There are eight Si atoms that are part of two different dimer rows of the 2×1 001 bare surface reconstruction. These Si are bridged with four O atoms; six-member and eight-member Si–O rings alternate along the interface. The eight interface Si atoms have two bonds to O atoms and two bonds to Si atoms in the channel. The model has parts of six 001 silicon layers below the partially oxidized Si. Si atoms in these channel layers are terminated with H. We represent the rigid crystal structure of the silicon channel by freezing all Si atoms three bonds (or more) away from the eight interface Si atoms, and from any dopant atom. All other atoms are geometrically optimized for each charge state, in order to understand the structural changes due to the presence or absence of carriers near the dopants.

The optimized undoped interface is intrinsically strained by the bridging oxygen groups. The distance between the two interface Si atoms sharing a bridging oxygen decreases by 0.64 Å. In the first Si layer below the interface, Si atoms are 0.037 Å off their normal lattice sites, and in the second layer, 0.004 Å. In our finite cluster interface model, a hole or electron at the undoped interface is represented by the geometrically optimized charged (positive cation and negative anion) structures. We find that the cation hole wave function is localized adjacent to the interface on the weakened Si–Si backbonds [Fig. 1(a)]. A similar localization occurs in 1–2 nm Si nanocrystals passivated on all sides with oxide.¹³ There is a very little geometrical change between the neutral and charged structures; neither electron nor hole breaks or strongly modifies chemical bonds despite the intrinsic strain. The lowest-unoccupied molecular orbital (LUMO) (not shown) also is spatially localized along the interface. Although the degree of localization depends on the details of the local interface structure, the strain near the interface will tend to localize the carriers in the channel of a FET adjacent to the interface, above and beyond the usual device electrostatics. It is also interesting to note that the interface highest-occupied molecular-orbital (HOMO)-LUMO optical transition in our model has a strongly allowed (direct-gap-like) oscillator strength of about 0.1; this contrasts with the indirect gap nature of the silicon channel. Previous calculations on thin silicon/(silicon dioxide) superlattices have also shown some direct-gap-like optical absorption.¹⁴

We first consider a substitutional P dopant bonded to four Si, in the 001 layer just below the oxidized Si layer [P(2) at position 2, Fig. 1(b)]. The optimized neutral structure exhibits a severe distortion from local tetrahedral geometry around P, with one very long 2.78 Å “broken” P–Si bond. The other three P–Si bonds are 2.33–2.34 Å. The long P–Si connects to the lower Si 001 layer at position 3. The extra electron from the P is spatially localized mostly on that Si atom [Fig. 1(b)]. This distorted geometry and trapped electron are far different than the normal substitutional P structure found in bulk Si or in H-passivated Si nanocrystals.¹⁵ The distortion and trapping we observe are caused by the oxide interface.

TABLE I. Relative energies of monodoped $\text{Si}_{61}\text{XH}_{52}\text{O}_{12}$.

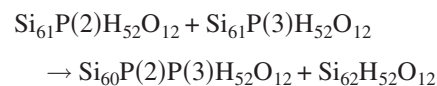
Dopant (position)	P(1)	P(2)	P(3)
Relative Energy (eV)	0.00	–2.20	–1.94
Dopant (position)	As(1)	As(2)	As(3)
Relative Energy (eV)	0.00	–1.68	–1.07
Dopant (position)	B(1)	B(2)	B(3)
Relative Energy (eV)	0.00	0.80	1.75
Dopant (position)	Al(1)	Al(2)	Al(3)
Relative Energy (eV)	0.00	1.44	1.45

In the cation structure, with the extra electron removed, tetrahedral bonding reforms around the P atom, with all four bonds in the range of 2.38–2.42 Å. The structural reorganization energy for the electron on and off the P atom is 0.60 eV. Within the context of standard electron trapping models,¹⁶ this Franck-Condon structural energy should create a significant barrier for the release of the electron, depending upon the relative electronic energy of the free and trapped electronic wave functions. In the negatively charged anion structure, corresponding to a second electron trapped at the P atom, the broken bond increases in length to 2.91 Å. The second electron reorganization energy is 0.26 eV. Calculations for the As(2) substitution give very similar results: large distortion in the neutral state, 0.61 eV reorganization energy for the cation, and 0.32 eV reorganization energy for the anion.

For P(3) (P substituted at position 3), two Si–Si bonds away from an oxidized Si atom, we find a less distorted structure. The two P–Si bonds pointing up towards the interface are elongated to 2.48 Å, and the two bonds pointing down are 2.46 Å. In the negative ion the distortion increases (2.54 and 2.47 Å), and in the cation the bond lengths go into the normal range (2.40 and 2.43 Å). The reorganization energy for the release of the extra electron into the channel is about 0.21 eV—one-third of the value for P(2). We would expect that P in the third 001 channel layer would be even closer to bulk structure.

Total-energy differences (Table I) show that neutral P dopant is energetically most stable at position 2. Further from the interface, the formation energy goes up modestly. Furthermore, in position 1, at the interface bonded directly to oxygen, the energy goes up by about 2.0 eV. This preference for P to bond to Si was also seen in the earlier DFT calculations.^{4,11} Si–O bonds are stronger than P–O bonds. For example, we calculate that $\text{SiH}_4 + \text{PH}_2(\text{OH})_2 \rightarrow \text{SiH}_2(\text{OH})_2 + \text{PH}_4$ is exothermic by 1.0 eV. At the interface, arsenic is also more stable when bonded to Si in position 2 (Table I).

We also investigated neutral P dimer structures at the interface because of the very high neutral P interface concentrations reported in FETs. The difference in the total energies of the geometrically optimized products and reactants in the reaction



is the P dimerization energy for P(2) plus P(3). We find that

the P–P nearest-neighbor neutral dimer is more stable than two separated P dopants by 1.75 eV, somewhat larger than in previous studies. In agreement with previous LDA studies,^{4,11} the dimer geometry is severely distorted with a long 3.02 Å P–P distance. We find that in the doubly ionized dimer, the local bonding returns to nearly tetrahedral with a 2.41 Å P–P distance. The complex of two P dopants with one intervening Si atom, P(2) plus P(2'), is also more stable than separated P dopants by 0.31 eV.

For hole doping with B or Al, the calculations show very different behavior than for electron doping with P or As. For B and Al at position 3, we see near tetrahedral-bonding geometry independent of charge state. In the neutral species the hole is partly spatially localized on two X–Si (X=B or Al) bonds pointing towards the interface [Fig. 1(c)]. The reorganization energy for the release of the hole is 0.27 eV for B(2), and only 0.09 eV for B(3). For Al(2), the reorganization energy is 0.39 eV.

However, the energetics (Table I) favor B directly bonded to oxygen in position 1, which is about 1.7 eV more stable than B bonded to Si in position 3. The B–O bond is stronger than the Si–O bond. For example, we calculate that $\text{BH}_4 + \text{SiH}_2(\text{OH})_2 \rightarrow \text{BH}_2(\text{OH})_2 + \text{SiH}_4$ is exothermic by 0.7 eV. For completeness, we note that the B dimer binding energy near the interface [i.e., B(2)–B(3)] is 0.85 eV relative to separated B dopants at position 2.

The severely distorted “broken bond” neutral P dopant in position 2 near the 001 oxide interface has a localized single electron which should be chemically reactive in the same way as dangling-bond oxide interface states. After the assembly of channel, oxide, and gate, commercial Si FETs are processed with forming gas at 200–400 °C to react interface dangling bonds with hydrogen. We explored reaction of the neutral P species in position 2 with a single H atom in three locations: on the backsides of both the P and Si atoms with the long distorted bond, and between the P and Si atoms. These three calculations converge to different stable isomeric structures and fully occupied lone pair states. The lowest-energy isomers involve H bonded to the Si. The H atom bound on the backside of Si is distorted very far from sp^3 with binding energy of 2.49 eV. If H is initially placed in the long distorted Si–P bond, it also bonds to this same Si atom, again giving a strongly distorted structure with binding energy of 2.30 eV. These binding energies are similar in magnitude to that for H atom passivating a Si dangling-bond state that at the undoped interface. This binding energy is about one-half the H_2 molecule bond energy; thus the reaction of H_2 with two such P centers is approximately thermo-neutral. This is to be compared to H incorporation in the perfect Si crystal, where H inserts into Si–Si bonds in bulk crystalline Si, forming Si–H–Si structures with substantial outward relaxation of the two Si atoms.¹⁷ This structure was proposed by Cox and Symons on chemical grounds.¹⁸ In $\text{Si}_{87}\text{H}_{76}$ nanocrystal, we converged a stable equidistant Si–H–Si structure next to the center Si atom. The optimized structure has relaxed Si atoms with a 3.3 Å Si–Si distance, very similar to the original bulk crystalline calculation. The H atom binding energy is negative (–0.25 eV), in contrast

with the large positive binding energies found above for the P structures near the oxide interface. So, H atoms should react first with the strained dopants; only at a much higher chemical potential they will insert into undisturbed Si–Si bonds in the channel.

In summary, our calculations suggest low electrical activity for P, As, B, and Al dopants near the Si(100)-oxide interface. Although isolated B and Al near the interface do give bulklike local bonding, formation of a dimer formation lowers the total energy and direct bonding of B or Al to oxygen at the interface gives the lowest total energy. In contrast, isolated P and As has the lowest energy when incorporated in the layer below the interface, not bonded to oxygen. However, both P and As have a strong tendency to form deactivated dimers. Furthermore, the strained local chemical bonding in isolated P or As leads to activation barriers (large reorganization energies) and creates increased chemical reactivity with hydrogen, leading to passivation. The situation is somewhat analogous to amorphous hydrogenated Si, which has distorted geometries and a high level of hydrogen. Here only about 10% of P and B dopants are active; hydrogen-terminated porous Si also has a low-doping efficiency.

We thank J. Bevk, M. Stavola, and D. V. Lang for informative discussion and correspondence. This work has been supported by the Department of Energy, Basic Energy Sciences, under DEFG0298ER14861 and DEFG0290ER14162. This work was partially supported by the Nanoscale Science and Engineering Initiative of the National Science Foundation under NSF Award No. CHE-0117752 and by the New York State Office of Science, Technology, and Academic Research (NYSTAR).

¹P. A. Packan, *Science* **285**, 2079 (1999).

²P. Fahey, P. Griffin, and J. Plummer, *Rev. Mod. Phys.* **61**, 289 (1989).

³M. Oshima *et al.*, *J. Electron Spectrosc. Relat. Phenom.* **88**, 603 (1998); R. Kasnavi *et al.*, *J. Appl. Phys.* **87**, 2255 (2000).

⁴J. Dabrowski *et al.*, *J. Vac. Sci. Technol. B* **18**, 2160 (2000).

⁵A. D. Becke, *J. Chem. Phys.* **98**, 5648 (1993); K. Raghavachari, *Theor. Chem. Acc.* **103**, 361 (2000).

⁶J. Muscat *et al.*, *Chem. Phys. Lett.* **342**, 397 (2001).

⁷J. K. Perry *et al.*, *Phys. Rev. B* **65**, 144501 (2002); K. N. Kudin *et al.*, *Phys. Rev. Lett.* **89**, 266402 (2002); J. Heyd and G. E. Scuseria, *J. Chem. Phys.* **121**, 1187 (2004); X. B. Feng and N. M. Harrison, *Phys. Rev. B* **69**, 132502 (2004); D. Munoz *et al.*, *ibid.* **69**, 085115 (2004).

⁸JAGUAR 5.0, Schrodinger (L.L.C., Portland, OR, 1991–2003).

⁹W. R. Wadt and P. J. Hay, *J. Chem. Phys.* **82**, 284 (1985).

¹⁰A. Bongiorno *et al.*, *Phys. Rev. Lett.* **90**, 186101 (2003); J. H. Oh *et al.*, *Phys. Rev. B* **63**, 205310 (2001); A. Pasquarello *et al.*, *Nature (London)* **396**, 58 (1998).

¹¹J. Dabrowski *et al.*, *Phys. Rev. B* **65**, 245305 (2002).

¹²Y. Tu and J. Tersoff, *Phys. Rev. Lett.* **84**, 4393 (2000). See also R. Buczko, S. Pennycook, and S. Pantelides, *ibid.* **59**, 213 (1987) for a similar model.

¹³Z. Y. Zhou *et al.*, *Nano Lett.* **3**, 163 (2003); Z. Y. Zhou *et al.*, *J. Am. Chem. Soc.* **125**, 15599 (2003).

¹⁴P. Carrier *et al.*, *Phys. Rev. B* **65**, 165339 (2002).

¹⁵Z. Y. Zhou *et al.*, *Phys. Rev. B* **71**, 245308 (2005).

¹⁶C. H. Henry and D. V. Lang, *Phys. Rev. B* **15**, 989 (1977); R. A. Marcus and N. Sutin, *Biochim. Biophys. Acta* **811**, 265 (1985); B. K. Ridley, *Quantum Processes in Semiconductor*, 2nd ed. (Oxford, London, 1988), Chap. 6.

¹⁷C. G. Vandewalle *et al.*, *Phys. Rev. B* **39**, 10791 (1989).

¹⁸S. F. J. Cox and M. C. R. Symons, *Chem. Phys. Lett.* **126**, 516 (1986).